Supplement of Biogeosciences, 16, 4765–4781, 2019
https://doi.org/10.5194/bg-16-4765-2019-supplement


Biogeosciences Open Access EGU

*Supplement of*

# Major role of ammonia-oxidizing bacteria in $N_2O$ production in the Pearl River estuary

**Li Ma et al.**

*Correspondence to:* Yao Zhang (yaozhang@xmu.edu.cn)

**Table S1** In situ biogeochemical parameters at the incubation experiment sites.

| Site_Layer | Temperature ($^{o}$C) | DO ($\mu$mol $L^{-1}$) | $NH_4^+$ ($\mu$mol $L^{-1}$) | $NO_3^-$ ($\mu$mol $L^{-1}$) | $NO_2^-$ ($\mu$mol $L^{-1}$) |
|---|---|---|---|---|---|
| P05_S | 30 | 61.3 | 40.1 | 126.1 | 20.5 |
| P05_B | 30 | 54.7 | 33.3 | 123.5 | 24.5 |
| P01_S | 29 | 30.9 | 167.2 | 84.0 | 11.9 |
| P01_B | 29 | 30.0 | 166.5 | 82.0 | 11.6 |

S, surface; B, bottom.

**Table S2** Isotopic composition of $N_2O$ during bacterial and archaeal ammonia oxidation, bacterial nitrifier-denitrification, and bacterial denitrification.

| Pathway | Microorganisms | Species | Substrate | $\delta^{15}N\text{-}N_2O$ | References |
|---|---|---|---|---|---|
| Ammonia oxidation | $\beta$-proteobacteria | *Nitrosomonas europaea* | $NH_4^+$ | −68–−60‰ | Yoshida, 1988; Toyoda et al., 2017 |
| | | | $NH_4^+$ | −46.9–−46.1‰ | Sutka et al., 2006 |
| | | | $NH_4^+$ | −19.88 ±0.39‰ | Jung et al., 2014 |
| | | *Nitrosomonas* marina C-113a | $NH_4^+$ | −54.9–−15.2‰ (0.5% $O_2$)[a] | Frame and Casciotti, 2010 |
| | | | $NH_4^+$ | −13.6–−6.7‰ (20% $O_2$)[a] | |
| | $\gamma$-proteobacteria | *Methylomonas methanica* | $NH_4^+$ | −39.4‰ | Mandernack et al., 2009 |
| | Archaea | CN25 (marine) | $NH_4^+$ | 6.3–10.2‰ | Santoro et al., 2011 |
| | | MY1 (soil) | $NH_4^+$ | −13.53 ±2.12‰ | Jung et al., 2014 |
| | | MY2 (soil) | $NH_4^+$ | −16.96 ±1.81‰ | Jung et al., 2014 |
| | | MY3 (soil) | $NH_4^+$ | −16.49 ±2.18‰ | Jung et al., 2014 |
| | | JG1 (soil) | $NH_4^+$ | −15.32 ±0.16‰ | Jung et al., 2014 |
| | | AR (marine sediment) | $NH_4^+$ | −12.91 ±1.50‰ | Jung et al., 2014 |

| | | | | | |
|---|---|---|---|---|---|
| | | CS (acid mine) | $NH_4^+$ | −35.54 ±0.89‰ | Jung et al., 2014 |
| Hydroxylamine oxidation[b] | *β*-proteobacteria | *Nitrosomonas europaea* | $NH_2OH$ | −38.1–−20.4‰ | Sutka et al., 2003 |
| | | | $NH_2OH$ | −5.5–5.1‰ | Sutka et al., 2006 |
| | | | $NH_2OH$ | −34.0–−13.8‰ | Yamazaki et al., 2014 |
| | | *Nitrosospira multiformis* | $NH_2OH$ | −3.9–1.7‰ (Average −0.3 ±2.9‰) | Sutka et al., 2006 |
| | | *Nitrosomonas* marina C-113a | $NH_2OH$ | −6.7‰ | Frame and Casciotti, 2010 |
| | *γ*-proteobacteria | *Nitrosococcus oceani* | $NH_2OH$ | −17.9–−5.8‰ | Yamazaki et al., 2014 |
| | | *Methylococcus capsulatus* | $NH_2OH$ | −0.3–1.7‰ (Average 0.0±1.2‰) | Sutka et al., 2003 |
| | | | $NH_2OH$ | 1.3–5.2‰ (Average 3.4±1.9‰) | Sutka et al., 2006 |
| Nitrifier-denitrification | *β*-proteobacteria | *Nitrosomonas* marina C-113a | $NO_2^-$ | −57.6±4.1‰ | Frame and Casciotti, 2010 |
| | | *Nitrosomonas europaea* | $NO_2^-$ | −39.1–−31.0‰ (Average −34.8 ±2.7‰) | Sutka et al., 2003 |
| | | *Nitrosospira multiformis* | $NO_2^-$ | −24.2–−21.5‰ (Average −22.9 ±0.6‰) | Sutka et al., 2006 |
| Denitrification | *γ*-proteobacteria | *Pseudomonas fluorescens* | $NO_3^-$ | −37.2–−14.9‰ | Toyoda et al., 2005 |
| | *α*-proteobacteria | *Paracoccus denitrificans* | $NO_3^-$ | −20.0–−7.9‰ | Toyoda et al., 2005 |

1 [a]$O_2$ conditions of the incubation experiments.

[b]Although the $\delta^{15}N\text{-}N_2O$ when using $NH_2OH$ as a substrate are listed here, the isotopic composition of $N_2O$ only when using $NH_4^+$ as a substrate was discussed in natural environments.

## References


Frame, C. H., and Casciotti, K. L.: Biogeochemical controls and isotopic signatures of nitrous oxide production by a marine ammonia-oxidizing bacterium, Biogeosciences, 7, 2695–2709, 2010.

Jung, M. Y., Well, R., Min, D., Giesemann, A., Park, S. J., Kim, J. G., and Rhee, S. K.: Isotopic signatures of $N_2O$ produced by ammonia-oxidizing archaea from soils, ISME J., 8, 1115–1125, 2014.

Mandernack, K. W., Mills, C. T., Johnson, C. A., Rahn, T., and Kinney, C.: The $\delta^{15}N$ and $\delta^{18}O$ values of $N_2O$ produced during the co-oxidation of ammonia by methanotrophic bacteria, Chem. Geol., 267, 96–107, 2009.

Santoro, A. E., Buchwald, C., McIlvin, M. R., and Casciotti K. L.: Isotopic Signature of $N_2O$ Produced by Marine Ammonia-Oxidizing Archaea, Science, 333, 1282–1285, 2011.

Sutka, R. L., Ostrom, N. E., Ostrom, P. H., Gandhi, H., and Breznak, J. A.: Nitrogen isotopomer site preference of $N_2O$ produced by Nitrosomonas europaea and Methylococcus capsulatus Bath, Rapid Commun. Mass Spectrom., 17, 738–745, 2003.

Sutka, R. L., Ostrom, N. E., Ostrom, P. H., Breznak, J. A., Gandhi, H., Pitt, A. J., and Li, F.: Distinguishing Nitrous Oxide Production from Nitrification and Denitrification on the Basis of Isotopomer Abundances, Appl. Environ. Microbiol., 72, 638–644, 2006.

Toyoda, S., Mutobe, H., Yamagishi, H., Yoshida, N., Tanji, Y.: Fractionation of $N_2O$ isotopomers during production by denitrifier, Soil. Biol. Biochem., 37, 1535–1545, 2005.

Toyoda, S., Yoshida, N., and Koba, K.: Isotopocule analysis of biologically produced nitrous oxide in various environments, Mass Spectrom. Rev., 36, 135–160, 2017.

Yamazaki, T., Hozuki, T., Arai, K., Toyoda, S., Koba, K., Fujiwara, T., and Yoshida,

N.: Isotopomeric characterization of nitrous oxide produced by reaction of enzymes extracted from nitrifying and denitrifying bacteria, Biogeosciences, 11, 2679–2689, 2014.

Yoshida, N.: $^{15}N$-depleted $N_2O$ as a product of nitrification, Nature, 335, 528–529, 1988.

**Table S3** The abundances of DNA- and cDNA-based *amo*A gene and the $N_2O$ production net rates and yields normalized to total *amo*A gene copy or transcript numbers of AOA and AOB in a given sample at the incubation experiment sites.

| Site_ Layer | DNA-based AOB (All) (copies $L^{-1}$) | DNA-based AOA (All) (copies $L^{-1}$) | $N_2O$ production rates (All) (fmol $cell^{-1}$ $h^{-1}$) | $N_2O$ yields (All) ($10^{-6}$) | DNA-based AOB (PA) (copies $L^{-1}$) | DNA-based AOA (PA) (copies $L^{-1}$) | $N_2O$ production rates (PA) (fmol $cell^{-1}$ $h^{-1}$) | $N_2O$ yields (PA) ($10^{-6}$) | cDNA-based AOB (PA) (copies $L^{-1}$) | cDNA-based AOA (PA) (copies $L^{-1}$) | $N_2O$ production rates (PA) (fmol $cell^{-1}$ $h^{-1}$) | $N_2O$ yields (PA) ($10^{-6}$) |
|---|---|---|---|---|---|---|---|---|---|---|---|---|
| P05_S | 14030 | 34427 | 23.70 | 21.30 | 12125 | 29082 | 27.90 | 25.00 | 382928 | 138646 | 2.20 | 1.97 |
| P05_B | 87915 | 397740 | 2.90 | 3.25 | 77820 | 357308 | 3.24 | 3.63 | 89559 | 12559 | 13.80 | 15.50 |
| P01_S | 19623 | 642905 | 0.91 | 1.93 | 9343 | 578974 | 1.02 | 2.18 | 500 | 461578 | 1.30 | 2.77 |
| P01_B | 21334 | 251163 | 5.91 | 5.47 | 16458 | 221184 | 6.77 | 6.27 | 362 | 7436 | 206.00 | 191.00 |

S, surface; B, bottom; All, sum of particle-attached and free-living fractions; PA, particle-attached fraction.

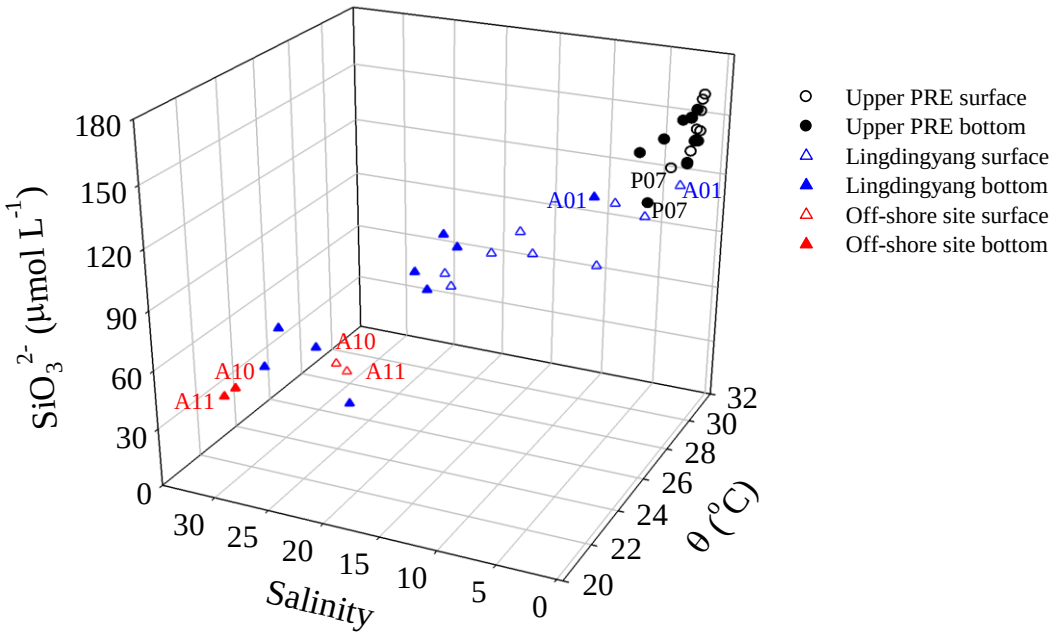


**Figure S1**: Three-dimensional scatter plot of potential temperature (θ) (°C), salinity, and silicate ($SiO_3^{2-}$) concentration. PRE, Pearl River Estuary.